J. Braz. Chem. Soc., Vol. 15, No. 5, 760-766, 2004.
Printed in Brazil - ©2004 Sociedade Brasileira de Química
0103 - 5053 $6.00+0.00

Article

Hydrogenation of 2-Ethyl-hexen-2-al on Ni/Al_2O_3 Catalysts

Arthur R.J.M. Mattos[a], Sônia H. Probst[a], Júlio C. Afonso[b] and Martin Schmal*[,c]

[a]*Instituto de Química, Universidade Federal de Santa Catarina, 88040-900 Florianópolis - SC, Brazil*

[b]*Instituto de Química, Universidade Federal do Rio de Janeiro, CP 68563, 21949-900 Rio de Janeiro - RJ, Brazil*

[c]*Núcleo de Catálise, COPPE, Universidade Federal do Rio de Janeiro, CP 68502, 21945-970 Rio de Janeiro - RJ, Brazil*

Este trabalho descreve a hidrogenação do 2-etil-hexen-2-al em um reator de lama em fase líquida sobre catalisadores Ni/Al_2O_3 (teor de Ni entre 4,4-17,0% p/p). Resultados de DRX, DRS e TPR mostraram a presença de espécies superficiais de Ni^{2+} em coordenação octaédrica (óxido de níquel superficial) e tetraédrica (fases do tipo espinélio) nas subcamadas do suporte. Nas amostras com altos teores de Ni, foram observados cristalitos de óxido de níquel, seja em coordenação octaédrica ou tetraédrica. A maior seletividade para a formação do intermediário 2-etil-hexanal foi obtida com o catalisador contendo 7,3% p/p de Ni. A freqüência de reação (TOF) independe da concentração de níquel, sugerindo que esta reação de hidrogenação é insensível à estrutura.

This work describes the hydrogenation of 2-ethyl-hexen-2-al in a slurry bed reactor in liquid phase on Ni/Al_2O_3 catalysts (4.4-17.0% wt Ni). XRD, DRS and TPR results showed the presence of superficial Ni^{2+} species in octahedral (surface Ni oxide) and tetrahedral coordination (spinel-type phase) in the subsurface of the support. Nickel oxide crystallites were found in samples with Ni content above 7.3%, either in tetrahedral or octahedral coordination. The highest selectivity for 2-ethyl-hexanal was obtained with the catalysts containing 7.3% wt Ni. The turnover frequency (TOF) was independent on the Ni concentration, suggesting that this hydrogenation reaction is structure insensitive.

Keywords: 2-ethyl-hexen-2-al, 2-ethyl-hexanal, Ni/Al_2O_3, slurry bed reactor

Introduction

Hydrogenation of 2-ethyl-hexen-2-al is one of the steps of the industrial synthesis of 2-ethyl-hexan-1-ol. In this reaction the main intermediate product is 2-ethyl-hexanal (Figure 1) and the final product is 2-ethyl-hexan-1-ol. The latter is very important for commercial applications, such as preparation of elastics and flexible frots of poly(vinyl acetal) and the manufacture of antioxidants for polymers and lubricant oils.

The reaction has been studied and reported in the literature. The experiments are conducted either in the liquid[1-4] or in the gas phase.[5-8] The main goal is to favor the selectivity and conversion of the raw chemical to the saturated alcohol. As a general trend 2-ethyl-2-hexen-1-ol is scarcely found in the reaction products, and its reactivity may account for this phenomenon.[4,8] Formation of

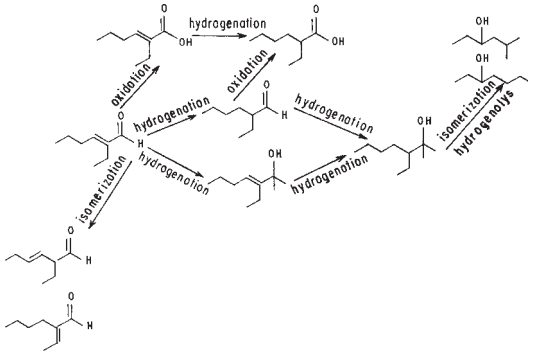

Figure 1. General routes for conversion of 2-ethyl-hexen-2-al according to literature data.

byproducts and intermediate compounds from 2-ethyl-hexen-2-al hydrogenation depends on experimental conditions and catalyst, which, however, has not been discussed in detail. Souza Aguiar and Schmal[1] determined the influence of the feed composition, the reaction temperature, the volumetric hydrogen flow and the nature

* e-mail: schmal@peq.coppe.ufrj.br

of the catalyst on the unsaturated aldehyde conversion in the liquid phase on Ni catalysts. The initial reaction rate increased with increasing catalyst mass, volumetric hydrogen flow and reaction temperature. The increase of the initial rate was followed by a decrease in the selectivity.

Several catalysts have been employed in this reaction. In general, Ni-based samples are used, but some other systems, such as Pd/Al_2O_3,[7,8] $[HCo(CO)_4]$[5] have also been tested. Ni-containing catalysts can be either monometallic or bimetallic. Almeida *et al*.[3] studied this reaction in the liquid phase in a semi-batch slurry reactor at atmospheric pressure. They showed that among all Ni catalysts the Ni/SiO_2 was the most selective for the saturated alcohol, while Ni/γ-alumina was the most active. Among the bimetallic Ni containing samples the most active and selective was the Ni-Cr catalyst.

The kinetics of 2-ethyl-2-hexen-2-al hydrogenation seems to be of first order, according to Macho and Polievko[7] and Trifel *et al*.[5] despite the very different experimental conditions (gas phase versus hydroformilation conditions).

Hydrogenation of other α-, β-unsaturated aldehydes, such as chrotonaldehyde. has also received some attention. Noller and Lin[9] studied this reaction in the gas phase on a $Ni\text{-}Cu/Al_2O_3$ bimetallic catalyst. A yield of 54.0% wt of crotolytic alcohol was obtained. The presence of a second metal was necessary to increase selectivity towards this alcohol. It was suggested that a $Cu^{\delta-}$ - $Ni^{\delta+}$ dipole was formed, thus favoring the C=O hydrogenation. Raab and Lercher[10] studied the activity and selectivity of $Ni\text{-}Pt/SiO_2$ catalysts for hydrogenation of chrotonaldehyde in the gas phase. The major product obtained was butyraldehyde in all tests. Addition of nickel to the Pt/SiO_2 system lead to an increase of hydrogenation rate of crotonaldehyde to crotolytic alcohol and butyraldehyde. The C=O hydrogenation selectivity reached a maximum for $Ni_{50}Pt_{50}$. This study suggested that platinum presents a slightly negative charge in the PtNi alloy. The bimetallic Ni-Pt sites increased the interaction between the carbonyl group and favored the hydrogenation to crotylic alcohol.

The main objective of this work was to study the influence of the Ni loading and the nature of the support of Ni/Al_2O_3 catalysts on the aldehyde hydrogenation and the characterization of the catalyst. The latter one was studied using spectroscopic measurementes in order to determine the structural properties of nickel oxide.

Experimental

Catalyst preparation

Two γ-alumina supports were used with two different crystalline grades γ-alumina/A (higher crystalline grade) and γ-alumina/B, according to Chen *et al*.[11] The catalysts were prepared by wet impregnation method using 50.0 mL of an aqueous solution of $Ni(NO_3).6H_2O$. Concentrations were adjusted in order to obtain catalysts with different Ni contents (4.0-17.0% wt). The suspension was stirred for 24 h (room temperature) and then dried under vacuum at 343 K. The impregnated support was calcined in a furnace at 573 K during 4h and then at 773 K during 1h (under air at atmospheric pressure).

Catalytic tests

Hydrogenation of 2-ethyl-hexen-2-al was performed in the liquid phase in a slurry reactor at atmospheric pressure.[3] The activation, performed *in situ* before the reaction in the same reactor, was carried out under hydrogen flow (15 L h^{-1}) at 673 K, for 20 h. The reactor was then cooled down and adjusted to the reaction temperature (403 K) under nitrogen flux. The reagent was introduced in the reactor under hydrogen flux (50 L h^{-1}). After stabilization of the temperature, hydrogen flow rate was adjusted to 100 L h^{-1}. 1 mL samples were taken from time to time from the reactor and injected in a gas chromatograph or in a GC-MS system (Shimadzu GC MS 20000A model, using a carbowax 20M 50 m capillary column, under the following conditions: injector temperature; 523 K; initial temperature; 313 K; final temperature; 473 K; heating rate; 4 K min^{-1}; injection volume; 0.2 μL). A commercial $Ni\text{-}Cr/SiO_2$ catalyst was used as a reference.

Characterization

X-ray diffraction (XRD). Crystalline phase and crystalline grade of the supports were determined in a Joel model 6BX-8P diffractometer (i = 20ma; V= 40KV; radiation source Cu-Kα, angular range 2-70^o).

B.E.T surface area. The specific area of the supports and of the catalysts were determined in an ASAP V2.04 equipment, using physical N_2 adsorption, following the B.E.T method.

Metal content. The nickel content was determined in a Perkin Elmer AAS 3300 atomic absorption spectrometer (λ = 232 nm, I = 25 ma, air/acetylene flame). Samples were prepared by dissolving 100 mg of catalyst in 1000 mL of H_2SO_4 (1:1).

Diffuse reflectance spectroscopy (DRS). The oxide species present in the supported catalysts were determined in a DRS VARIAN CARY 5 spectrometer (sweeping range - 180-799 nm; the support was used as a reference). The metallic oxides were identified by comparison between samples and standard spectra.

Temperature programmed reduction (TPR). The reduction of the catalysts was performed in a temperature-programmed equipment. The procedure is described elsewhere.[12,13] The experimental conditions were: reducing mixture, H_2/Ar (1.75 vol, 30 mL min^{-1}); heating rate, 10 K min^{-1}; final temperature, 1173 K; sample weight, 20 mg.

Dynamic chemisorption. The metallic area, dispersion and average crystallite diameter of the catalysts were determined by the dynamic chemisorption method.[13] The experiments were performed in a TPR equipment using the same catalyst activation conditions prior to reaction. It was assumed that the occupied area by a nickel atom is 6.33A°[2] and the Ni/H atomic ratio is equal to 1.

Results and Discussion

Catalyst characterization

BET results (Table 1) show that the samples prepared using the support with higher crystalline grade (A) presented smaller surface areas after impregnation than the support itself, particularly for the NSA-2 sample (9.0% wt Ni).

Table 1. Ni content (% wt) and B.E.T. surface area of the catalysts

Sample	Ni (% wt)	$S_{B.E.T.}$ (m^2 g^{-1})
γ-Al_2O_3/A	-	199
γ-Al_2O_3/B	-	183
NSA-1/A	4.4	186
NSA-2/A	9.0	142
NSA-3/A	17.0	170
NSA-5/B	8.4	185
NSA-6/A	7.3	173
NSS (10.0% wt SiO_2; Ni; 1.5% wt Cr)	10.0	22

X-ray diffraction

XRD patterns of the catalysts are presented in Figure 2. NiO crystallites were observed for samples containing at least 7.3% wt Ni (Figures 2b, 2c and 2d). For the 4.4% wt Ni catalyst, NiO crystallites were not detected (Figure 2a). In addition nickel aluminate was not observed. This is probably due to the low calcination temperature. Lo Jacono *et al.*[14] only observed nickel aluminates on a 7.5% wt NiO sample after calcination at 873 K.

Diffuse reflectance spectroscopy

Ni/γ-Al_2O_3 catalysts exhibited d-d transition bands above 350 nm (Figure 3). The 4.4% wt Ni sample showed

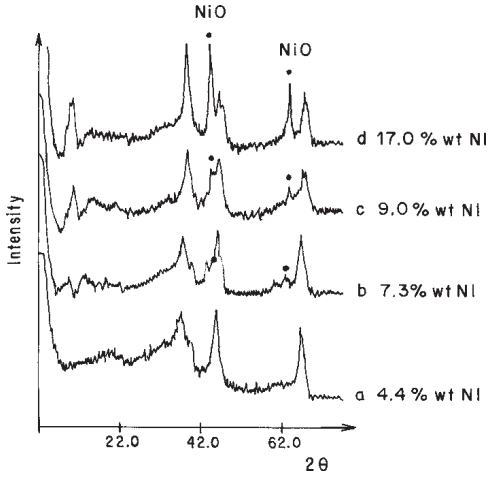

Figure 2. X-ray diffraction data of the Ni/Al_2O_3 catalysts.

a doublet band of Ni^{2+} with maximum peaks at 599 and 637 nm, which are attributed to the tetrahedral coordination. Also a band at 417 nm appeared, which characterizes an octahedral coordination of Ni^{2+} at the surface. The Ni^{2+} in tetrahedral coordination is characteristic of an amorphous spinel-phase species or spinel at subsurfaces, according to Schaffer *et al.*[15] and Stumbo *et al.*[12] Subsurface spinel phase is usually formed at high temperatures (above 925 K) by diffusion through the support. However, spinel phases at subsurface were also observed on catalysts calcined at lower temperatures, due to the slow diffusion of Ni over NiO crystallite surface for samples with high Ni content. This explains why spinels were not detected in XRD data. Stumbo *et al.*[12] observed similar Ni^{2+} surface species in both octahedral coordination and spinel phase after calcination at 773 K.

The catalysts containing 9.0 and 17.0% wt Ni showed NiO crystallites, (380, 420 and 720 nm, see Figure 3). These bands overlap the corresponding bands of Ni^{2+} in octahedral coordination at the surface and in the tetrahedral

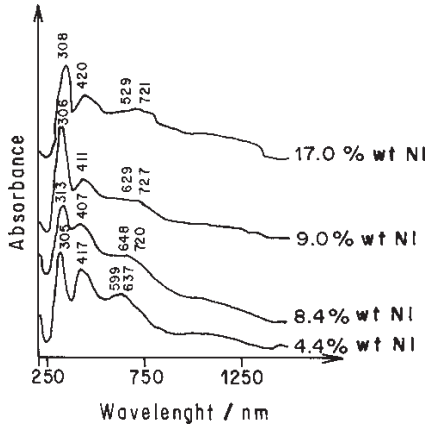

Figure 3. DRS spectra of Ni/Al_2O_3 catalysts.

coordination at the subsurface, in agreement with Stumbo *et al*.[12]

Temperature programmed reduction

Figure 4 displays the TPR profiles of all catalysts, showing at least three zones at 723, 903 and above 1073 K. It is important to notice that refractory Ni^{2+} species were formed, which are very difficult to reduce.[16] The first peak at 723 K corresponds to NiO reduction for 9.0 and 17.0% wt Ni catalysts. The 4.4% wt Ni sample only presents a small shoulder in this region, in accordance with the literature.[13]

The second peak around 903-923 K was observed for the 4.4% wt and 9.0% wt Ni catalysts, while this peak was shifted to lower temperatures (about 873 K) for the 17.0% wt Ni sample. This is attributed to the presence of Ni^{2+} species at the surface in the octahedral coordination, which are highly dispersed, interacting strongly with the support as observed by Moujlin *et al*.[17] and De Bokx[18] for similar concentrations.

The third peak zone appeared at higher temperatures (1073-1173 K) for the 4.4% wt and 9.0% wt Ni catalysts, and again it was shifted to lower temperatures (973-1073 K) for the 17.0% wt Ni sample. This peak is attributed to Ni^{2+} species in tetrahedral coordination, which characterizes a spinel structure and corresponds to nickel aluminate, which is highly refractory. DRS data confirmed the presence of this spinel structure. Moreover, the peak shift for the 17.0% wt Ni catalyst is explained as a catalytic effect of Ni^0 after reduction of the Ni^{2+} species due to the reduction of NiO, according to De Bokx *et al*.[19]

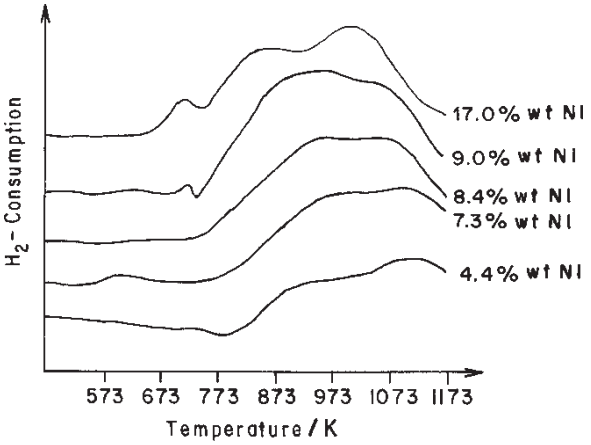

Figure 4. TPR data of Ni/Al_2O_3 catalysts.

After the reduction step (up to 823 K) the 17.0% wt Ni catalyst was oxidized with O_2 (5% v/v)/He at room temperature, and a second reduction was performed from room temperature up to 1073 K. It turns out that the first peak was much more intense, indicating the presence of more NiO, probably due to the conversion of Ni^{2+} species in the octahedral coordination to NiO. Kubelkova *et al*.,[20] Zielinski[21] and Lamber and Ekloff[22] observed similar behavior using the TPR technique.

Dynamic chemisorption

The metallic area, dispersion and average diameter of crystallites were calculated as shown in Table 2, assuming complete reduction with exception of the NSA-1 catalyst. This sample presents a spinel phase, absence of NiO and incomplete reduction.

Among the catalysts prepared using support A (higher crystalline grade) the 7.3% wt Ni catalyst presented the highest metallic area and dispersion, decreasing for higher loadings. The average crystallite diameter presented an opposite behavior. This shows clearly the effect of the presence of Ni^{2+} species at the surface and NiO crystallites, as well as nickel aluminate species, depending on the Ni loading. Before reduction, XRD results showed poor NiO peaks and well defined Ni^{2+} species in octahedral coordination at the surface, in good agreement with the TPR results. Therefore, it seems that these surface species are responsible for the higher dispersion and greater metallic surface area, in accordance with Zielinski.[21]

Table 2. Characterization data for the dynamic chemisorption

Catalyst	S_{METAL} ($m^2\ g^{-1}$ Ni)	Dispersion (%)	Crystallite diameter (A°)
NSA-1 (A-4.4% wt Ni)	46.75	7.00	14.46
NSA-2 (A-9.0% wt Ni)	49.20	7.38	13.71
NSA-3 (A-17.0% wt Ni)	44.73	6.67	15.17
NSA-5 (B-8.4% wt Ni)	36.48	5.47	18.50
NSA-6 (A-7.3% wt Ni)	62.90	9.45	10.71
NSS	26.00	3.90	25.90

Catalytic tests

It is important to stress that reduction conditions used before the catalytic test were selected to maximize nickel reduction.[23] Table 3 shows the reaction rates (r) calculated as a function of the formation of the intermediate product of 2-ethyl-hexen-2-al conversion (2-ethyl hexanal). The initial reaction rate increased with Ni loading but reached a maximum value for the 9.0% wt Ni catalyst at 403 K. For higher Ni loading (17.0% wt Ni) the reaction rate did not change significantly.

The selectivity for 2-ethyl-hexanal decreased with increasing Ni content. Figures 5 and 6 present the molar

Table 3. Initial reaction rates for 2-ethyl-hexen-2-al conversion and the corresponding turnover numbers

Catalyst	Reaction temperature (K)	Initial rate (r_{HAL}) (gmol g^{-1} Ni $min^{-1} \times 10^2$)	Turnover frequency
NSA-1 (A-4.4% wt Ni)	403	1.11	0.155
NSA-2 (A-9.0% wt Ni)	403	2.27	0.300
NSA-3 (A-17.0% wt Ni)	403	2.35	0.344
NSA-5 (B-8.4% wt Ni)	413	0.55	0.100
NSA-6 (A-7.3% wt Ni)	393	1.02	0.100
NSA-6 (A-7.3% wt Ni)	413	3.10	0.321
NSS	403	0.82	0.200

percentage curves of 2-ethyl-hexanal with time and the selectivity with the conversion.

The influence of the support on 2-ethyl-hexanal formation is shown in Figures 7 and 8. The catalysts with the support A displayed better activity and selectivity. The turnover number was approximately constant, changing by a factor not higher than 1.5, which, according to Boudart,[24] suggests that this reaction is structure insensitive.

The selectivity for 2-ethyl-hexanal varied with the Ni content, reaching a maximum for the 7.3% wt Ni catalyst. Probably, the Ni^{2+} species in the octahedral coordination favors the selectivity, which can be attributed to an electronic effect (donor-acceptor electron capacity), due to the interaction of the carbonyl group with the surface charge density of Ni^{2+} surface species function.

Zielinski[21] has already observed a relationship between

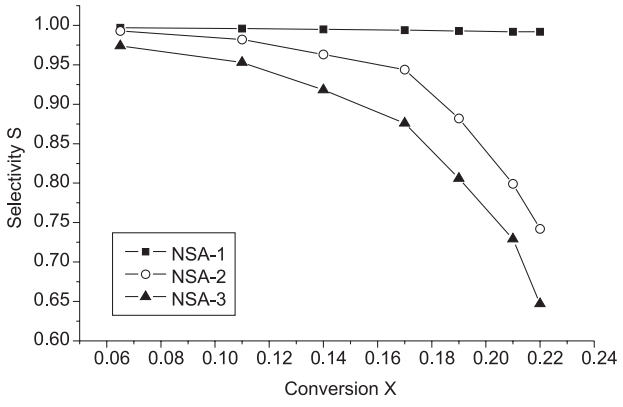

Figure 5. Molar percentage curves for 2-ethyl-hexanal versus time on some Ni/Al_2O_3 catalysts.

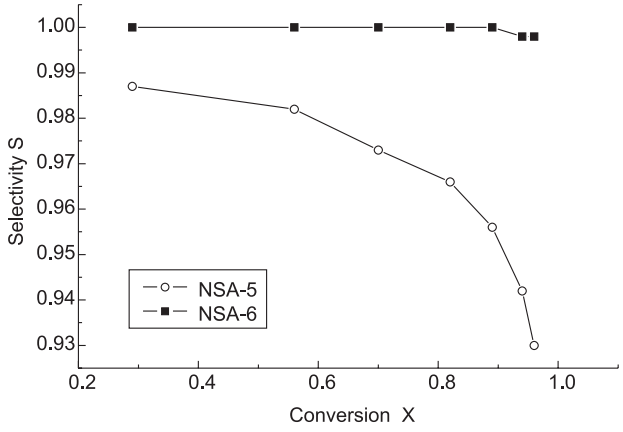

Figure 7. Influence of the crystallinity on 2-ethyl-hexanal formation.

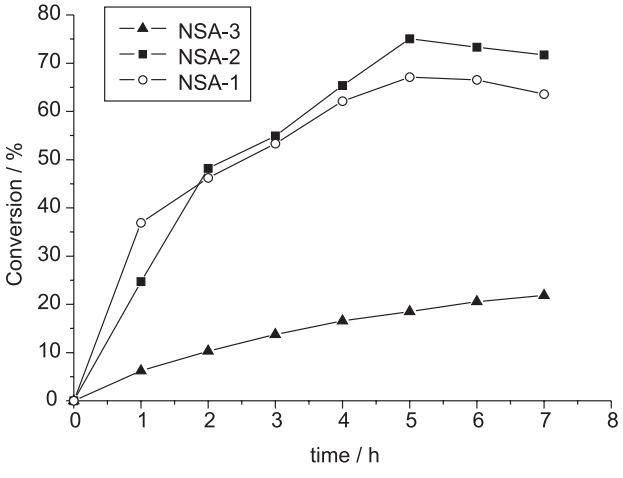

Figure 6. Molar percentage curves for 2-ethyl-hexanal versus conversion of 2-ethyl-hexen-2-al on some Ni/Al_2O_3 catalysts.

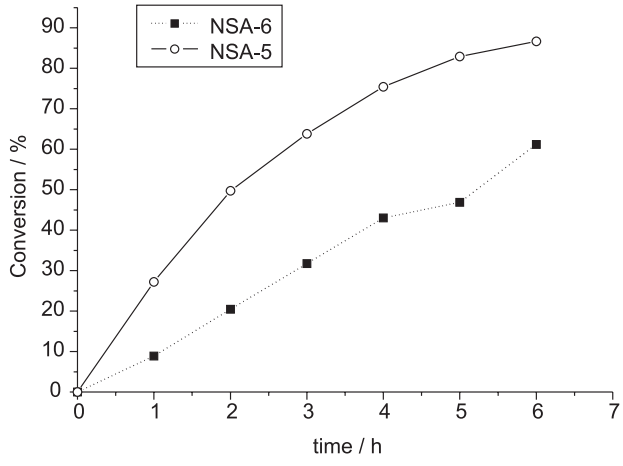

Figure 8. Influence of the crystallinity on 2-ethyl-hexanal selectivity.

Table 4. Products found on 2-ethyl-hexen-2-al conversion at 403 K (reaction time: 3 hours; GC-MS data[a])

Products	NSA-1 (A-4.4% wt Ni)	NSA-3 (A-17.0% wt Ni)
reactant	70.7	40.2
2-ethyl-hexen-1-ol (minor intermediate product)	Not detected	0.1
2-ethyl-hexanal (major intermediate product)	11.3	32.8
2-ethyl-hexan-1-ol (final product)	Not detected	6.2
2-butyl-buten-2-al (isomerization of the carbon chain)	6.0	3.2
5-methyl-hexen-3-al (unknown reaction)	1.1	0.2
2-ethyl-hexanoic acid (oxidation of the saturated aldehyde)	Not detected	5.2
2-ethyl-hexen-2-oic acid (oxidation of the unsaturated aldehyde)	Not detected	5.4
Unidentified products	10.9	6.7

[a] obtained by simple integration of peak areas of the chromatograms.

the acceptor sites and the Ni^{2+} species in the octahedral coordination. Reduction favors the formation of Ni crystallites, modifying the surface properties of nickel. Kubelkova *et al.*[20] observed from the CO adsorption on Ni/Al_2O_3 the presence of a considerable amount of Ni^0 after reduction in addition to nickel crystallites decorated with nickel aluminate crystallites. The Ni^{+d} sites are located at the border between metallic nickel and nickel aluminate, which are attributed to the electron deficiency induced by the oxygen.

Chen *et al.*[11] observed that the increase of the alumina crystallinity favored formation of surface nickel species instead of incorporating nickel into the support.

Chemical analysis of the reaction products

Table 4 lists several byproducts found in the hydrogenation of 2-ethyl-hexen-2-al. In addition to isomerization, hydrogenation and hydrogenolysis byproducts, two carboxylic acids were detected for the 17.0% wt Ni sample: 2-ethyl-hexen-2-oic and 2-ethyl-hexanoic. These oxidation byproducts are probably the result of catalytic action of NiO particles covered by the Ni^{2+} species in octahedral sites species at the surface. The results obtained after reduction and oxidation steps showed the presence of NiO encapsulated by pseudo spinel-like species. Data reported by Christoskova *et al.*,[25] using oxide nickel systems for oxidation of organic compounds, suggest that the oxygen from NiO crystal structure was responsible for the oxidation of the organic compounds.

NiO is easily reduced to Ni^o, therefore, intermediates can be activated on Ni^o sites, which are responsible for intermediate reactions because NiO cannot be the intermediate for such reactions.[18]

Conclusions

Characterization of Ni/γ-alumina by DRX, DRS and TPR showed the presence of crystalline and amorphous nickel oxide, superficial Ni^{2+} oxide in octahedral symmetric sites and Ni^{2+} species in tetrahedral symmetric sites in the subsurface of the support, characterizing a spinel-type phase.

The presence of crystalline nickel oxide covered by a layer of nickel oxide species at the surface either as octahedral sites or as spinel phase in the catalyst explains the effect of Ni concentration on the reaction rate and selectivity, showing that the 7.3% wt Ni catalyst exhibits the best performance. On the other hand, the presence of nickel oxide particles in the reduced 17.0% wt Ni catalyst can explain the oxidation by-products found during conversion of 2-ethyl-hexen-2-al and 2-ethyl-hexanal to their respective carboxylic acids.

The turnover frequency was independent on the Ni concentration, suggesting that this hydrogenation reaction is structure insensitive.

Acknowledgements

A. R. M. J. Mattos acknowledges CAPES and CNPq for fellowships. The authors are grateful to CNPq for financial support.

References

1. Souza Aguiar, E. F.; Schmal, M.; *Proceedings of the 7th Ibero-American Symposium on Catalysis*, Mar Del Plata, Argentina, 1980, 159-168.
2. Upadysheva, A.; Zaitseva, Z. V.; Zel'manova, Z. I.; Likhina, A. S.; Kashnikov, A. M.; Znamenskaya, A. D.; *Zh. Prikl. Khim.* **1976**, *49*, 688. (*CA 85: 45901r*).
3. Almeida, J. L.; Dieguez, L. C.; Schmal, M.; *Proceedings of the 9th Ibero-American Symposium on Catalysis,* Lisbon, Portugal, 1984, vol. 1, 751-760.
4. Collins, D. J.; Grimes, D. F.; Davis, B. H.; *Can. J. Chem. Eng.* **1983**, *61*, 36.
5. Trifel, A. G.; Kagna, S. Sh; Pavlova, V. A.; *Gidroformilirovanie* **1972**, 71. (*CA 77: 151232t*).

6. Niklasson, C.; Smedler, G.; *Ind. Eng. Chem. Res.* **1987**, *26*, 403.
7. Macho, V.; Polievko, M.; *Chem. Prum*. **1969**, *19*, 215. (*CA 71: 60372g*).
8. Malgala, R. V.; Chaudhari, R. V.; *Ind. Eng. Chem. Res*. **1999**, *38*, 906.
9. Noller, H.; Lin, W. M.; *React. Kinet. Catal. Lett*. **1982**, *21*, 479.
10. Raab, G. C.; Lercher, J. A.; *J. Mol. Catal*. **1992**, *75*, 71.
11. Chen, S. L.; Zhang, H. L.; Hu, J.; Contescu, C.; Schwarz, J. A.; *Appl. Catal*. **1991**, *73,* 289.
12. Stumbo, A. M.; Schmal, M.; *Proceedings of the 12th Ibero-American Symposium on Catalysis*, Rio de Janeiro, Brazil, 1990, vol. II, 613-624.
13. da Silva Junior, A. F.; Salim, V. M. M.; Schmal, M.; Fréty, R.; *Stud. Surf. Sci. Catal.* **1991**, *63,* 123.
14. Lo Jaconi, M.; Schhiavello, A.; Cimino, J.; *J. Phys. Chem*. **1971**, *75*, 1044.
15. Schaffer, B.; Heijeinga, J. J.; Moulijn, J. A.; *J. Phys. Chem*. **1987**, *91*, 4752.
16. Bartholomew, C. A.; Farrauot, R. J.; *J. Catal.* **1976**, *45*, 45.
17. Hoffer, B. W.; van Langeveld, A. D.; Janssens, J. P.; Bonné, R. L. C.; Lok, C. M.; Moulijn, J. A.; *J. Catal.* **2000**, *192*, 432.
18. De Bokx, P. K.; *J. Catal.* **1987**, *104*, 86.
19. De Bokx, P. K.; Wassenberg, B. A.; Geus, J. W.; *J. Catal.* **1976**, *45*, 41.
20. Kubelkova, L.; Nováková, J.; Jaeger, N. I.; Schulz-Ekloff, G.; *Appl. Catal. A* **1993**, *95*, 87.
21. Zielinski, J.; *J. Catal*. **1982**, *76*, 157.
22. Lamber, R.; Ekloff, G. S.; *Surf. Sci.* **1989**, *258*, 107.
23. Raddi, L. R. A.; Dieguez, L. C.; Fréty, R.; Schmal, M.; *Proceedings of the 11th Ibero-American Symposium on Catalysis*, Mexico City, Mexico, 1988, vol. 2, 1195-1199.
24. Boudart, M.; *Chem. Ver*. **1995**, *95*, 661.
25. Christoskova, St. G.; Danova, A.; Georgiera, M.; Argirov, O. K.; Mehandzhier, D.; *Appl. Catal. A* **1995**, *128*, 219.

Received: November 4, 2003
Published on the web: September 27, 2004